HHS Public Access

Author manuscript

Int J Cardiovasc Imaging. Author manuscript; available in PMC 2020 April 01.

Published in final edited form as:

Int J Cardiovasc Imaging. 2019 April ; 35(4): 683–693. doi:10.1007/s10554-018-1500-4.

Tissue-Based Markers of Right Ventricular Dysfunction in Ischemic Mitral Regurgitation Assessed via Stress Cardiac Magnetic Resonance and Three-Dimensional Echocardiography

Jiwon Kim, MD[1], **Javid Alakbarli, MD**[1], **Brian Yum, MD**[1], **Nathan H. Tehrani, MD**[5], **Meridith P. Pollie, BS**[1], **Christiane Abouzeid, MD**[1], **Antonino Di Franco, MD**[1], **Mark B. Ratcliffe, MD**[2], **Athena Poppas, MD**[3], **Robert A. Levine, MD**[4], **Richard B. Devereux, MD**[1], and **Jonathan W. Weinsaft, MD**[1]

[1]Greenberg Cardiology Division/Department of Medicine, Weill Cornell Medical College (New York, NY)

[2]Division of Cardiology, Department of Surgery, University of California, San Francisco; Department of Bioengineering, University of California, San Francisco; Veterans Affairs Medical Center (San Francisco, CA)

[3]Lifespan Cardiovascular Institute, The Warren Alpert Medical School of Brown University (Providence, RI)

[4]Massachusetts General Hospital, Harvard Medical School (Boston, MA)

[5]Weill Cornell Medicial College

Abstract

Purpose—Ischemic mitral regurgitation (iMR) augments risk for right ventricular dysfunction (RV_{DYS}). Right and left ventricular (LV) function are linked via common coronary perfusion, but data is lacking regarding impact of LV ischemia and infarct transmurality – as well as altered preload and afterload – on RV performance.

Methods—In this prospective multimodality imaging study, stress CMR and 3-dimensional echo (3D-echo) were performed concomitantly in patients with iMR. CMR provided a reference for RV_{DYS} (RVEF<50%), as well as LV function/remodeling, ischemia and infarction. Echo was used to test multiple RV performance indices, including linear (TAPSE, S'), strain (GLS), and volumetric (3D-echo) approaches.

Results—90 iMR patients were studied; 32% had RV_{DYS}. RV_{DYS} patients had greater iMR, lower LVEF, larger global ischemic burden and inferior infarct size (all $p<0.05$). Regarding injury pattern, RV_{DYS} was associated with LV inferior ischemia and infarction (both $p<0.05$); 80% of affected patients had substantial viable myocardium (<50% infarct thickness) in ischemic inferior segments. Regarding RV function, CMR RVEF similarly correlated with 3D-echo and GLS (r=0.81–0.87): GLS yielded high overall performance for CMR-evidenced RV_{DYS} (AUC: 0.94), nearly equivalent to that of 3D-echo (AUC: 0.95). In multivariable regression, GLS was

Address for Correspondence: Jiwon Kim, MD, Assistant Professor of Medicine, Weill Cornell Medical College, 525 East 68th Street, New York, NY 10021, Phone: (212) 746-9929, Fax: (212) 746-3010, jik9027@med.cornell.edu.

independently associated with RV volumetric dilation on CMR (OR −0.90 [CI −1.19 – −0.61], p<0.001) and 3D echo (OR −0.43 [CI −0.84 – −0.02], p=0.04).

Conclusions—Among patients with iMR, RV_{DYS} is associated with potentially reversible processes, including LV inferior ischemic but predominantly viable myocardium and strongly impacted by volumetric loading conditions.

Keywords

right ventricle; valvular heart disease; echocardiography; magnetic resonance imaging (MRI); remodeling

Introduction

Ischemic mitral regurgitation (iMR) provides a nidus for right ventricular dysfunction (RV_{DYS}) due to an array of factors – including increased RV afterload due to valvular regurgitation and left ventricular (LV) dilation, as well as impaired contractility due to ischemia and/or infarction: Common coronary blood supply[1] facilitates use of regional LV perfusion deficits as surrogate markers for RV ischemia. Whereas iMR and RV_{DYS} are well associated with myocardial infarction (irreversible injury), prior work has also suggested that both can be induced by myocardial ischemia – a potentially reversible condition. Regarding the RV, our research has shown LV perfusion deficits on radionuclide single-photon emission computed tomography (SPECT) to be associated with RV_{DYS},[2] although uncertainty persists as to whether observed associations were attributable to infarction or profound ischemia. Other studies have shown CAD patients to manifest exercise-induced RV functional impairments,[3, 4] suggesting a link between ischemia and RV_{DYS}. Given that ischemic but viable myocardium offers a rationale for revascularization that can improve LV contraction, and that RV_{DYS} has been linked to symptoms and mortality,[2, 5] further clarity as to impact of LV ischemia on RV performance is of substantial importance.

Cardiac magnetic resonance (CMR) provides volumetric quantification of ventricular structure and function and is widely used as a reference for RV_{DYS}. Stress CMR adjunctively enables assessment of LV perfusion; results have been shown to be superior to conventional methods (i.e. SPECT) for obstructive CAD.[6] Delayed enhancement CMR uniquely allows evaluation of infarct transmurality, including subendocardial infarcts in regions of predominantly viable myocardium. Prior studies have yielded variable results concerning associations between LV infarction and RV_{DYS},[7–9] suggesting that RV_{DYS} may stem from factors other than infarct alone. However, ischemia and infarct transmurality have not been examined as concomitant markers of RV_{DYS}. Moreover, whereas CMR has been used to validate other modalities such as echocardiography (echo), relative performance of newly available volumetric echo techniques for assessment of RV performance in iMR are incompletely understood.

This study assessed CMR-evidenced LV perfusion and infarct transmurality among a prospectively enrolled cohort of iMR patients to test links between ischemic but viable LV myocardium and RV_{DYS}. Secondary goals were to assess utility of echo-derived indices of RV performance as alternative markers of RV_{DYS} on CMR, and to test RV afterload and

remodeling (quantified by both CMR and echo) as physiologic determinants of RV_{DYS} in iMR.

Material and Methods

Study Population

The population comprised patients prospectively enrolled in a multimodality imaging protocol examining structural predictors of iMR. Eligible patients had functional mitral regurgitation (MR) (≥mild) on echo and were being considered for invasive angiography based on suspected/known obstructive coronary artery disease (CAD) or prior abnormal stress test. Patients with primary MR (prolapse, rheumatic heart disease), mitral valve replacement, or contraindications to contrast-enhanced CMR (e.g. GFR<30 mL/min/1.73m^2, ferromagnetic implants) were excluded; those with contraindications to, or self-determined refusal of, regadenoson infusion underwent CMR without adjunctive stress testing. In all patients, comprehensive demographic data were collected using standardized questionnaires, including cardiac risk factors and medications.

This study was conducted with approval of the Weill Cornell Medical College Institutional Review Board; written informed consent was obtained at time of enrollment.

Imaging Protocol

Echo and perfusion CMR were performed within a 3-day (96% same day) interval using a standardized image acquisition protocol:

CMR—CMR was performed using 3.0 Tesla scanners (General Electric [Waukesha, WI]). Cardiac chamber volumes were assessed via cine-CMR (steady state free precession), which included long axis (2, 3, 4) as well as contiguous short axis slices acquired from the atrio-ventricular (tricuspid and mitral valve) annuli through the LV and RV apices that were quantified at end-diastole and end-systole for calculation of LV and RV ejection fraction (EF); RV myocardial mass was measured at end-diastole in accordance with established methods employed by our group.[10] Myocardial perfusion was assessed via regadenoson (0.4 mg) pharmacological stress, for which LV short axis images (4–5, evenly distributed from base-apex) were acquired using a gradient echo pulse sequence: Ischemia was assessed based on peak myocardial signal intensity during first-pass gadolinium infusion, for which perfusion deficits were defined based on a discrete signal intensity deficit that persisted at least 4 cardiac cycles during peak LV blood pool enhancement.[11] Myocardial infarction was assessed using an inversion recovery pulse sequence, which was acquired 10–30 minutes post-gadolinium (0.2 mmol/kg) in spatial orientations matched to cine-CMR. LV ischemia and infarction were co-localized via a standard AHA/ACC 17 segment model; MI size (% myocardium) was measured based on regional transmural extent of enhancement (based on mid-point of each affected segment) in accordance with prior methods applied by our group and others.[12, 13]

Echocardiography—Transthoracic echoes were acquired using commercial equipment (Philips iE33 [Andover, MA]). RV morphology and function were independently quantified via multiple established approaches:[14]

- Tricuspid annular plane systolic excursion (TAPSE) and RV systolic excursion velocity (S') were acquired in accordance with American Society of Echocardiography (ASE) guidelines; established cutoffs (TAPSE<1.6cm, S'<10cm/s) were used to define RV_{DYS} by each parameter.[2, 15] Corresponding linear indices of RV size included basal width (maximal transverse diameter) and length (maximal diameter from tricuspid annulus to apex) in apical 4-chamber orientation.[14]
- RV global longitudinal strain (GLS) was quantified in an RV focused apical view; images were acquired at a frame rate of 60–90 Hz with inclusion of the entire RV free wall. GLS was derived using commercial software (TomTEC [Munich, Germany]), for which automated border detection was manually adjusted to ensure optimal tracking throughout the cardiac cycle. In accordance with prior literature, RV_{DYS} was defined as GLS<20%.[16]
- RV 3D volumes were quantified in a full volume RV focused view; data were acquired over 4 cardiac cycles and processed using above noted dedicated software: 3D RV end-diastolic and end-systolic datasets included chamber volumes inclusive of the RV inflow and outflow tracts as respectively bordered by the tricuspid and pulmonic annuli. Corresponding to CMR, RV_{DYS} on 3D echo was defined as RVEF<50%.[10, 17]

Quantitative analyses were also performed to assess adjunctive indices relevant to RV remodeling and iMR. MR was quantified using regurgitant fraction as well as aggregate severity (5 point scale) based on additional parameters including vena contracta, volumetric indices, jet depth, and mitral and pulmonary vein flow patterns.[18] Pulmonary artery systolic pressure (PASP) was calculated from tricuspid regurgitant velocity and inferior vena cava caliber. LV function, size, and mass were quantified via linear dimensions, consistent with methods validated in prior necropsy-comparison and outcomes studies.[19, 20] Echo analyses were performed blinded to CMR results.

RV wall stress was quantified using an established formula[10, 21], which incorporates RV end systolic chamber volume (ESV), PASP and RV myocardial volume:

$$\text{RV wall stress} = \frac{\text{PASP} * \text{RVESV}}{\text{RV myocardial volume}}$$

Statistical Methods

Comparisons between groups were made using Student's t-test (expressed as mean ± standard deviation) for continuous variables. Categorical variables were compared using Chi-square or, when fewer than 5 expected outcomes per cell, Fisher's exact test. Bivariate correlation coefficients, as well as regression analyses were used to evaluate univariable associations between continuous variables: Multivariate modeling was performed via

logistic regression, for which CMR and echo indices were tested as continuous variables. Diagnostic test performance of echo-derived RV functional variables was tested in relation to CMR-quantified RVEF was assessed using receiver operating characteristics (ROC) curves. Statistical calculations were performed using SPSS 22.0 (SPSS Inc. [Chicago, IL]). Two-sided $p<0.05$ was considered indicative of statistical significance.

Results

Population Characteristics

The population comprised 90 patients with iMR who underwent echo and CMR within a maximal interval of 3 days (95% within 1 day), among whom 32% (n=29) had RV_{DYS}.

Table 1 details clinical and imaging characteristics of the population, as well as comparisons between patients with and without RV_{DYS}. As shown, patients with RV_{DYS} were similar with respect to systemic hemodynamic indices and clinical history of prior coronary revascularization but were more likely to report symptoms of dyspnea, have advanced (New York Heart Association [NYHA] class) heart failure, and require loop diuretics (all $p<0.05$).

MRI Tissue Properties as Markers of RV Dysfunction

Table 1 also reports CMR functional indices among patients with and without RV_{DYS}; corresponding tissue characterization indices are reported in Table 2. As shown, RV_{DYS} was associated with a trend towards larger global LV injury as evidenced by global MI size (13.2±9.0 vs. 9.0±10.3%, p=0.06) with inferior MI occurring more commonly among those with RV_{DYS} (5.6±6.5 vs. 2.8±4.5, p=0.04). Similarly, LV global ischemic burden was higher among patients with RV_{DYS} (p=0.03), corresponding to lower LVEF (31.8±11.2 vs. 49.5±13.1%, p<0.001), greater MR (regurgitant fraction: 42.2±15.3 vs. 33.5±13.2%, p=0.02), and higher RV afterload as quantified by echo-evidenced PA systolic pressure (43.6±15.5 vs. 34.6±13.8 mmHg, p=0.01).

Regarding perfusion distribution, Table 2 also demonstrates that increased global LV ischemia among patients with iMR was predominantly attributable to larger inferior perfusion defects (p=0.03), with a similar albeit non-significant trend for lateral defects (p=0.1). Among patients with RV_{DYS} and inferior perfusion defects, two-thirds (68%) had admixed infarction in inferior segments. Regarding transmurality, most patients (80%, n=12) with RV_{DYS} and inferior ischemia had substantial viable (<50% wall thickness) myocardium within the LV inferior wall (mean infarct transmurality 25.1±25.0%). Assessed on a segmental basis, the majority of affected segments were non-transmural: basal inferior (80%), mid inferior (80%) and apical inferior (87%), again supporting the concept that ischemic but viable LV inferior territories are linked to RV_{DYS}. Figure 1 provides a representative example of inferior/inferoseptal perfusion defect in regions of predominantly viable myocardium.

Echo-Derived RV Volumetric and Functional Parameters

Figure 2 displays 2D (top) and 3D (bottom) echo indices of RV volumetric remodeling in relation to CMR-quantified RV volume. As shown, echo-derived RV 3D volumes yielded

higher magnitude of correlation (r=0.79–0.82) than did RV linear width and length (r=0.61–0.73).

Table 3 and Figure 3 show corresponding 2D linear (TAPSE, S') RV functional indices – together with 3D RVEF and GLS – in relation to presence and magnitude of CMR-quantified $RV_{DYS.}$ Whereas all echo parameters differed significantly between patients with and without RV_{DYS} ($p<0.05$), magnitude of difference was higher for GLS (12.3±4.3 vs. 21.2±3.5%, $p<0.001$) and 3D echo RVEF (41.4±8.4 vs. 57.4±6.1%, $p<0.001$) than for TAPSE (1.6±0.4 vs. 1.9±0.4 cm, $p=0.001$) or RV-S' (10.2±3.2 vs. 12.0±2.7 cm/s, $p=0.009$). By extension, 3D echo RVEF and GLS yielded similarly fold higher correlation coefficients with CMR RVEF (r=0.87, 0.81 respectively) than did TAPSE and S' (r=0.29, 0.42 respectively). Regarding direct comparisons, RVEF calculated by 3D echo yielded near equivalent results to that of CMR (52.3±10.1 vs. 52.8±12.0%, $p=0.37$), despite small, albeit statistically significant, echo under-estimations of CMR-evidenced RV end-diastolic (151.2±51.4 vs. 134.8±41.4 ml, $p<0.001$) and end-systolic (74.8±42.4 vs. 66.1±30.9 ml, $p=0.001$) volumes.

Improved correlations for 3D echo and GLS in relation to CMR-derived RVEF were accompanied by higher diagnostic test performance for RV_{DYS}: Figure 4 provides superimposed ROC curves for each echo variable in relation to the reference standard of CMR. As shown, 3D RVEF and 2D GLS yielded near equivalently high overall performance (AUC 0.95, 0.94), which was greater than that of S' (0.71) or TAPSE (0.75). Regarding individual performance parameters, data shown in Table 4 demonstrates that use of established echo-based cutoffs yielded slightly higher accuracy for 3D and strain (84%, 82%) than for S' and TAPSE (74%, 79%), which was primarily attributable to improved sensitivity (83–90% vs. 59–69%).

RV Strain in Relation to Volumetric Remodeling and Wall Stress

Given its above demonstrated utility as a marker of RV performance, GLS was tested in relation to loading conditions to determine physiologic determinants of impaired strain: Aggregate RV wall stress was over two-fold higher among patients with impaired GLS, reflecting increases in PA pressure and RV chamber volume as measured by 3D echo or CMR. As shown in Figure 5, prevalence of impaired GLS increased in RV end-systolic volume among all PA systolic pressure strata, and was 1.4–1.9-fold more common among patients in the highest (vs. those in the lowest) common tertiles of increased PA systolic pressure and RV end-systolic volume ($p<0.001$).

Table 5 reports multivariate analysis concerning RV wall stress components in relation to GLS. As shown, GLS was independently associated with RV volumetric dilation (OR −0.90 [CI −1.19 – −0.61], $p<0.001$), even after controlling for PA systolic pressure and RV myocardial mass. Substitution of echo-derived RV chamber volume and mass yielded similar results, demonstrating near identical magnitude of association between GLS and PA systolic pressure. Applied clinically, these results indicate that a 20 ml increment in RV volume would be expected to result in a 30% strain reduction among patients with iMR.

Discussion

This study provides new insights concerning altered LV tissue properties as a causal substrate for RV contractile dysfunction, as well as data supporting use of emerging echo techniques for RV assessment. Key findings are as follows: (1) Among a broad cohort with iMR, RV_{DYS} was common – occurring in nearly one third (32%) of patients – and was associated with clinical indices of heart failure severity, including NYHA class, dyspnea, and diuretic use. (2) RV_{DYS} varied in relation to regional LV tissue properties; inferior wall ischemia and infarction were greater in affected patients (both $p<0.05$) whereas corresponding anterior ischemia and infarct burden were similar (p=NS): Over three fourths (80%) of patients with RV_{DYS} and inferior perfusion defects had substantial viable myocardium within inferior wall segments. (3) Volumetric loading conditions impacted RV performance, as evidenced by higher aggregate wall stress among those with impaired strain (19.8±10.8 vs. 9.3±3.3 kPa, $p<0.001$) as well as decrements in strain paralleling increments RV chamber volume and PA systolic pressure ($p<0.001$).

This is the first study to our knowledge that supports a direct association between LV ischemia pattern and RV function. Our data is consistent with established physiologic concepts regarding common right and left ventricular coronary blood supply, such that LV perfusion deficits would be expected to reflect impaired oxygenation in neighboring RV territories resulting in RV_{DYS}. Consistent with this, animal studies have shown that acute reduction of coronary flow to the interventricular septum impairs LV and RV contractile function.[22] Acute inferior MI is a known causal substrate for reductions in RV function, [23] although infarct transmurality has not previously been tested. Our data are also supported by prior research using stress testing, which suggested links between abnormal LV perfusion on SPECT radionuclide imaging and RV_{DYS}.[2] Among patients with known or suspected CAD undergoing SPECT and echo, our prior work showed RV_{DYS} (defined via TAPSE and S') to be associated with inducible and fixed inferior/lateral LV perfusion defects.[2] However, this retrospective cohort utilized SPECT (known to yield lower spatial resolution than CMR) and did not include viability imaging, yielding uncertainty as to whether inducible perfusion defects partially reflected LV dilation associated artifacts, as well as to whether links between RV_{DYS} and fixed LV perfusion deficits were due to infarction or profound ischemia. Moreover, use of binary criteria for RV_{DYS} (via TAPSE, S') as was employed in our prior research enables limited insight into RV performance, providing a rationale for volumetric RV assessment (via CMR) as was performed in the current study.

Regarding RV contractility, our study also entailed comparison of 2D and 3D echo in relation to CMR, so as to test magnitude to which different echo indices reflect RV_{DYS} in context of CAD. Our data show that both 2D and 3D indices performed relatively well for binary assessment of RV_{DYS} (RVEF<50% via CMR), and that additive value of GLS and 3D echo RVEF was primarily related to stratification of magnitude of RV impairment. Limited data exist that directly compare conventional echo methods against 3D and strain techniques for the RV.[24, 25] Regarding direct comparisons, we note that prior studies have generally reported higher correlations between CMR and echo strain/3D imaging vs. linear parameters. However, these data have been limited by heterogeneity in patient population,

variable inclusion of both 3D and strain, and substantial time intervals between diagnostic imaging modalities. For example, Lu et al. reported that TAPSE and S' yielded 2-fold lower correlation with CMR than did 3D echo in a retrospective cohort of patients undergoing clinical imaging for a wide array of indications, prohibiting assessment of condition-specific determinants of RV performance.[24] In another retrospective cohort, Ishizu et al. compared CMR to echo strain/3D, but included patients with a wide range of conditions in whom imaging modalities were acquired up to 1 month apart, potentially explaining markedly lower correlations for TAPSE and S' (r=0.02–0.06, both p=NS) than were observed in our current study (r=0.29–42, both p<0.001).[26] Regarding iMR, our group has shown multiplanar linear strain (acquired in different orientations) to perform equivalently to one another, and superior to linear indices (TAPSE, S') for identification of RV_{DYS}.[9] However, lack of 3D echo prohibited volumetric echo assessment of RV performance as was entailed in this study. Our current finding – demonstrating near equivalence of GLS to volumetric indices (3D echo, CMR) – supports the general concept that iMR-associated RV_{DYS} is strongly influenced by regional RV impairments, reflected on carefully acquired 2D echo.

Given the utility of strain as a surrogate marker of RV function, our study also addressed physiologic determinants of strain impairment so as to better elucidate preload and afterload based mechanisms of RV_{DYS} in patients with iMR. Our findings demonstrate that similar to traditional RV functional indices, strain is a load-dependent measure of RV performance that relates to RV wall stress. Among wall stress components, RV volume, PA systolic pressure, and RV mass were associated with impaired strain in univariate analysis; multivariate modeling showed an independent association between strain and RV volume. The notion that strain is impacted by volume loading rather than solely pressure components is generally consistent with prior studies that have demonstrated MR-associated RV_{DYS} to be primarily associated with adverse LV remodeling and, to a lesser extent, PA pressure. For example, among patients with primary MR undergoing echo and radionuclide angiography, RV ejection fraction was weakly linked to PASP (r=0.24) and most strongly associated with LV septal function (r=0.49) with multivariable modeling demonstrating strongest association with LV septal function (β=0.42, p<0.001), followed by LV end-diastolic diameter index (β=−0.22, p=0.002), then PASP (β=−0.14, p=0.047).[27] These findings support the concept that volume overload associated with MR strongly influences RV function and that afterload only partially accounts for RV functional impairment in iMR.

Several limitations should be acknowledged. First, it is important to recognize that our cohort was comprised of iMR patients, and that findings regarding physiologic markers of RV_{DYS} (e.g. inferior ischemia) would not be expected to apply to patients with MR of differing etiologies. Similarly, data regarding a primary association between impaired strain and increased RV size would likely differ in other cohorts such as patients with primary pulmonary hypertension (PH), in whom afterload (rather than RV remodeling) would be expected to strongly impact strain. On the other hand, given that both RV dilation (due to LV dilation and/or ischemia) and increased afterload are both potentially modifiable via therapeutic intervention, the notion that strain can be impacted by potentially reversible phenomena is of broad importance.

In conclusion, our findings demonstrating RV_{DYS} to be strongly linked to ischemic but viable LV inferior myocardium and adverse volumetric loading conditions support the concept that RV_{DYS} in iMR is due to potentially reversible pathophysiologic mechanisms. Future studies are warranted to determine whether targeted interventions such as CMR-guided coronary interventions for ischemia reduction can be used to decrease RV chamber dilation, augment RV performance, and improve prognosis for patients with RV_{DYS}.

Abbreviations

ASE	American Society of Echocardiography
CAD	coronary artery disease
CI	confidence interval
CMR	cardiac magnetic resonance
Echo	echocardiography
ESV	end-systolic volume
EDV	end-diastolic volume
EF	ejection fraction
GLS	global longitudinal strain
iMR	ischemic mitral regurgitation
LV	left ventricle
MI	myocardial infarction
MR	mitral regurgitation
NYHA	New York Heart Association
PA	pulmonary artery
PH	pulmonary hypertension
ROC	receiver operating characteristics
RV	right ventricle
RV_{DYS}	right ventricular dysfunction
S'	systolic excursion velocity
SPECT	single-photon emission computed tomography
TAPSE	tricuspid annular plane systolic excursion

References

[1]. Klima UP, Guerrero JL, Vlahakes GJ. Myocardial perfusion and right ventricular function. Ann Thorac Cardiovasc Surg. 1999;5:74–80. [PubMed: 10332109]

[2]. Kim J, Di Franco A, Seoane T, Srinivasan A, Kampaktsis PN, Geevarghese A, et al. Right Ventricular Dysfunction Impairs Effort Tolerance Independent of Left Ventricular Function Among Patients Undergoing Exercise Stress Myocardial Perfusion Imaging. Circ Cardiovasc Imaging 2016;9.

[3]. Maddahi J, Berman DS, Matsuoka DT, Waxman AD, Forrester JS, Swan HJ. Right ventricular ejection fraction during exercise in normal subjects and in coronary artery disease patients: assessment by multiple-gated equilibrium scintigraphy. Circulation. 1980;62:133–40. [PubMed: 7379275]

[4]. Brown KA, Okada RD, Boucher CA, Strauss HW, Pohost GM. Right ventricular ejection fraction response to exercise in patients with coronary artery disease: influence of both right coronary artery disease and exercise-induced changes in right ventricular afterload. J Am Coll Cardiol. 1984;3:895–901. [PubMed: 6707356]

[5]. Sabe MA, Sabe SA, Kusunose K, Flamm SD, Griffin BP, Kwon DH. Predictors and Prognostic Significance of Right Ventricular Ejection Fraction in Patients With Ischemic Cardiomyopathy. Circulation. 2016;134:656–65. [PubMed: 27507405]

[6]. Greenwood JP, Maredia N, Younger JF, Brown JM, Nixon J, Everett CC, et al. Cardiovascular magnetic resonance and single-photon emission computed tomography for diagnosis of coronary heart disease (CE-MARC): a prospective trial. Lancet. 2012;379:453–60. [PubMed: 22196944]

[7]. Gorter TM, Lexis CP, Hummel YM, Lipsic E, Nijveldt R, Willems TP, et al. Right Ventricular Function After Acute Myocardial Infarction Treated With Primary Percutaneous Coronary Intervention (from the Glycometabolic Intervention as Adjunct to Primary Percutaneous Coronary Intervention in ST-Segment Elevation Myocardial Infarction III Trial). Am J Cardiol 2016;118:338–44. [PubMed: 27265672]

[8]. Larose E, Ganz P, Reynolds HG, Dorbala S, Di Carli MF, Brown KA, et al. Right ventricular dysfunction assessed by cardiovascular magnetic resonance imaging predicts poor prognosis late after myocardial infarction. J Am Coll Cardiol. 2007;49:855–62. [PubMed: 17320743]

[9]. Di Franco A, Kim J, Rodriguez-Diego S, Khalique O, Siden JY, Goldburg SR, et al. Multiplanar strain quantification for assessment of right ventricular dysfunction and non-ischemic fibrosis among patients with ischemic mitral regurgitation. PLoS One. 2017;12:e0185657. [PubMed: 28961271]

[10]. Kim J, Medicherla CB, Ma CL, Feher A, Kukar N, Geevarghese A, et al. Association of Right Ventricular Pressure and Volume Overload with Non-Ischemic Septal Fibrosis on Cardiac Magnetic Resonance. PLoS One 2016;11:e0147349. [PubMed: 26799498]

[11]. Klem I, Heitner JF, Shah DJ, Sketch MH, Jr., Behar V, Weinsaft J, et al. Improved detection of coronary artery disease by stress perfusion cardiovascular magnetic resonance with the use of delayed enhancement infarction imaging. J Am Coll Cardiol. 2006;47:1630–8. [PubMed: 16631001]

[12]. Cerqueira MD, Weissman NJ, Dilsizian V, Jacobs AK, Kaul S, Laskey WK, et al. Standardized myocardial segmentation and nomenclature for tomographic imaging of the heart. A statement for healthcare professionals from the Cardiac Imaging Committee of the Council on Clinical Cardiology of the American Heart Association. Circulation. 2002;105:539–42. [PubMed: 11815441]

[13]. Weinsaft JW, Kim J, Medicherla CB, Ma CL, Codella NC, Kukar N, et al. Echocardiographic Algorithm for Post-Myocardial Infarction LV Thrombus: A Gatekeeper for Thrombus Evaluation by Delayed Enhancement CMR. JACC Cardiovasc Imaging 2016;9:505–15. [PubMed: 26476503]

[14]. Lang RM, Badano LP, Mor-Avi V, Afilalo J, Armstrong A, Ernande L, et al. Recommendations for cardiac chamber quantification by echocardiography in adults: an update from the American Society of Echocardiography and the European Association of Cardiovascular Imaging. Eur Heart J Cardiovasc Imaging. 2015;16:233–70. [PubMed: 25712077]

[15]. Rudski LG, Lai WW, Afilalo J, Hua L, Handschumacher MD, Chandrasekaran K, et al. Guidelines for the echocardiographic assessment of the right heart in adults: a report from the American Society of Echocardiography endorsed by the European Association of Echocardiography, a registered branch of the European Society of Cardiology, and the Canadian Society of Echocardiography. J Am Soc Echocardiogr 2010;23:685–713; quiz 86–8. [PubMed: 20620859]

[16]. Lang RM, Badano LP, Mor-Avi V, Afilalo J, Armstrong A, Ernande L, et al. Recommendations for cardiac chamber quantification by echocardiography in adults: an update from the American Society of Echocardiography and the European Association of Cardiovascular Imaging. J Am Soc Echocardiogr. 2015;28:1–39 e14. [PubMed: 25559473]

[17]. Srinivasan A, Kim J, Khalique O, Geevarghese A, Rusli M, Shah T, et al. Echocardiographic linear fractional shortening for quantification of right ventricular systolic function-A cardiac magnetic resonance validation study. Echocardiography 2017;34:348–58. [PubMed: 28247463]

[18]. Zoghbi WA, Adams D, Bonow RO, Enriquez-Sarano M, Foster E, Grayburn PA, et al. Recommendations for Noninvasive Evaluation of Native Valvular Regurgitation: A Report from the American Society of Echocardiography Developed in Collaboration with the Society for Cardiovascular Magnetic Resonance. J Am Soc Echocardiogr 2017;30:303–71. [PubMed: 28314623]

[19]. Devereux RB, Alonso DR, Lutas EM, Gottlieb GJ, Campo E, Sachs I, et al. Echocardiographic assessment of left ventricular hypertrophy: comparison to necropsy findings. Am J Cardiol. 1986;57:450–8. [PubMed: 2936235]

[20]. Devereux RB, Roman MJ, Palmieri V, Liu JE, Lee ET, Best LG, et al. Prognostic implications of ejection fraction from linear echocardiographic dimensions: the Strong Heart Study. Am Heart J. 2003;146:527–34. [PubMed: 12947374]

[21]. Mauritz GJ, Vonk-Noordegraaf A, Kind T, Surie S, Kloek JJ, Bresser P, et al. Pulmonary endarterectomy normalizes interventricular dyssynchrony and right ventricular systolic wall stress. J Cardiovasc Magn Reson. 2012;14:5. [PubMed: 22240072]

[22]. Goldstein JA, Tweddell JS, Barzilai B, Yagi Y, Jaffe AS, Cox JL. Importance of left ventricular function and systolic ventricular interaction to right ventricular performance during acute right heart ischemia. J Am Coll Cardiol. 1992;19:704–11. [PubMed: 1538031]

[23]. Zornoff LA, Skali H, Pfeffer MA, St John Sutton M, Rouleau JL, Lamas GA, et al. Right ventricular dysfunction and risk of heart failure and mortality after myocardial infarction. J Am Coll Cardiol. 2002;39:1450–5. [PubMed: 11985906]

[24]. Lu KJ, Chen JX, Profitis K, Kearney LG, DeSilva D, Smith G, et al. Right ventricular global longitudinal strain is an independent predictor of right ventricular function: a multimodality study of cardiac magnetic resonance imaging, real time three-dimensional echocardiography and speckle tracking echocardiography. Echocardiography 2015;32:966–74. [PubMed: 25287078]

[25]. van der Zwaan HB, Geleijnse ML, McGhie JS, Boersma E, Helbing WA, Meijboom FJ, et al. Right ventricular quantification in clinical practice: two-dimensional vs. three-dimensional echocardiography compared with cardiac magnetic resonance imaging. Eur J Echocardiogr. 2011;12:656–64. [PubMed: 21810828]

[26]. Ishizu T, Seo Y, Atsumi A, Tanaka YO, Yamamoto M, Machino-Ohtsuka T, et al. Global and Regional Right Ventricular Function Assessed by Novel Three-Dimensional Speckle-Tracking Echocardiography. J Am Soc Echocardiogr 2017;30:1203–13. [PubMed: 29079046]

[27]. Le Tourneau T, Deswarte G, Lamblin N, Foucher-Hossein C, Fayad G, Richardson M, et al. Right ventricular systolic function in organic mitral regurgitation: impact of biventricular impairment. Circulation. 2013;127:1597–608. [PubMed: 23487435]

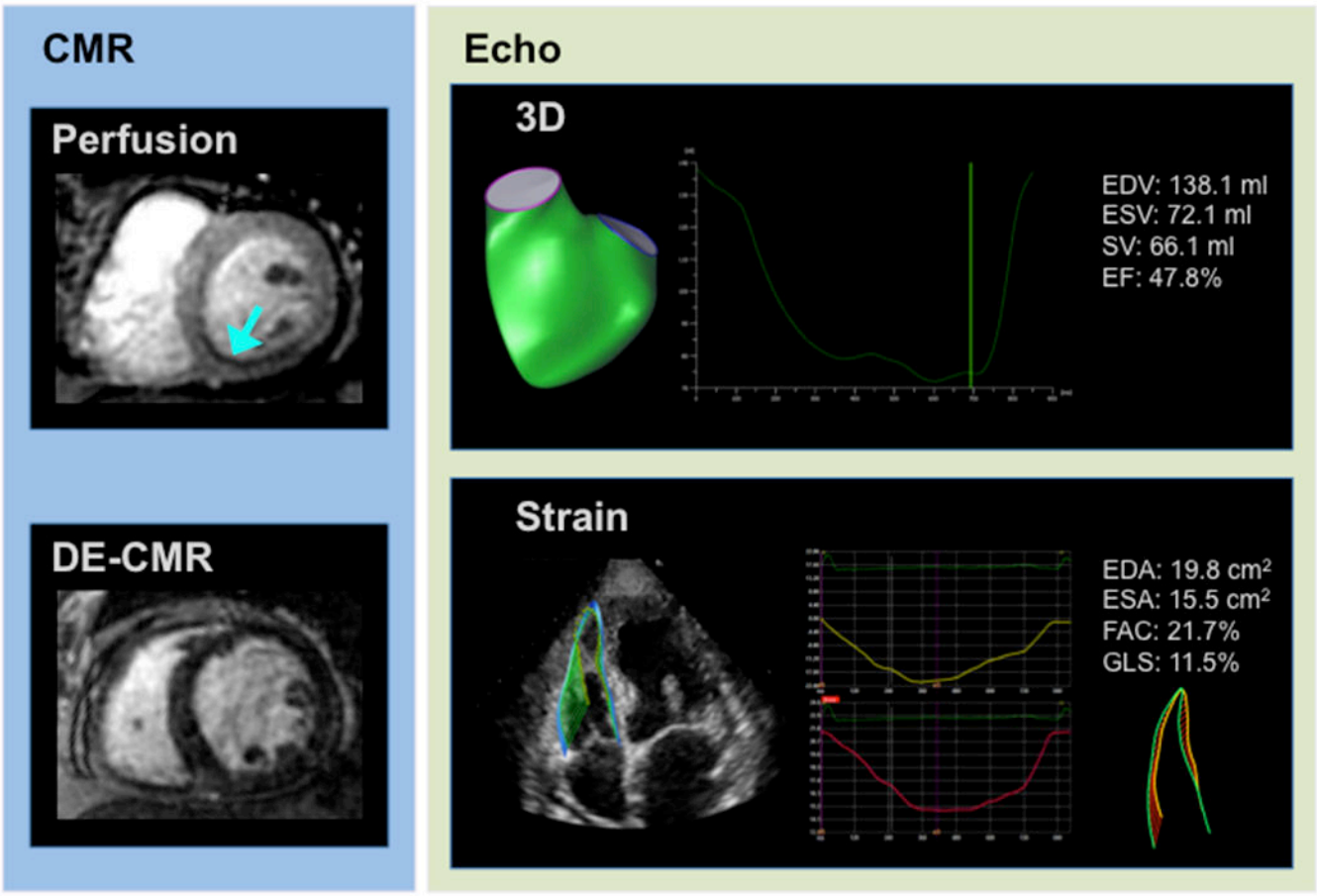

Figure 1. Tissue Characterization and Functional Assessment

Representative example of CMR-derived tissue characterization via stress perfusion (top left) and late gadolinium enhancement (bottom left), as well as echo-derived RV functional assessments via 3D volumetric quantification (top right) and GLS (bottom right) in a patient with RV_{DYS} on cine-CMR (RVEF=44%). Note inferior/inferoseptal ischemia on stress perfusion CMR (blue arrow) in region of predominantly viable myocardium on DE-CMR, paralleled by RV_{DYS} via both 3D echo and GLS.

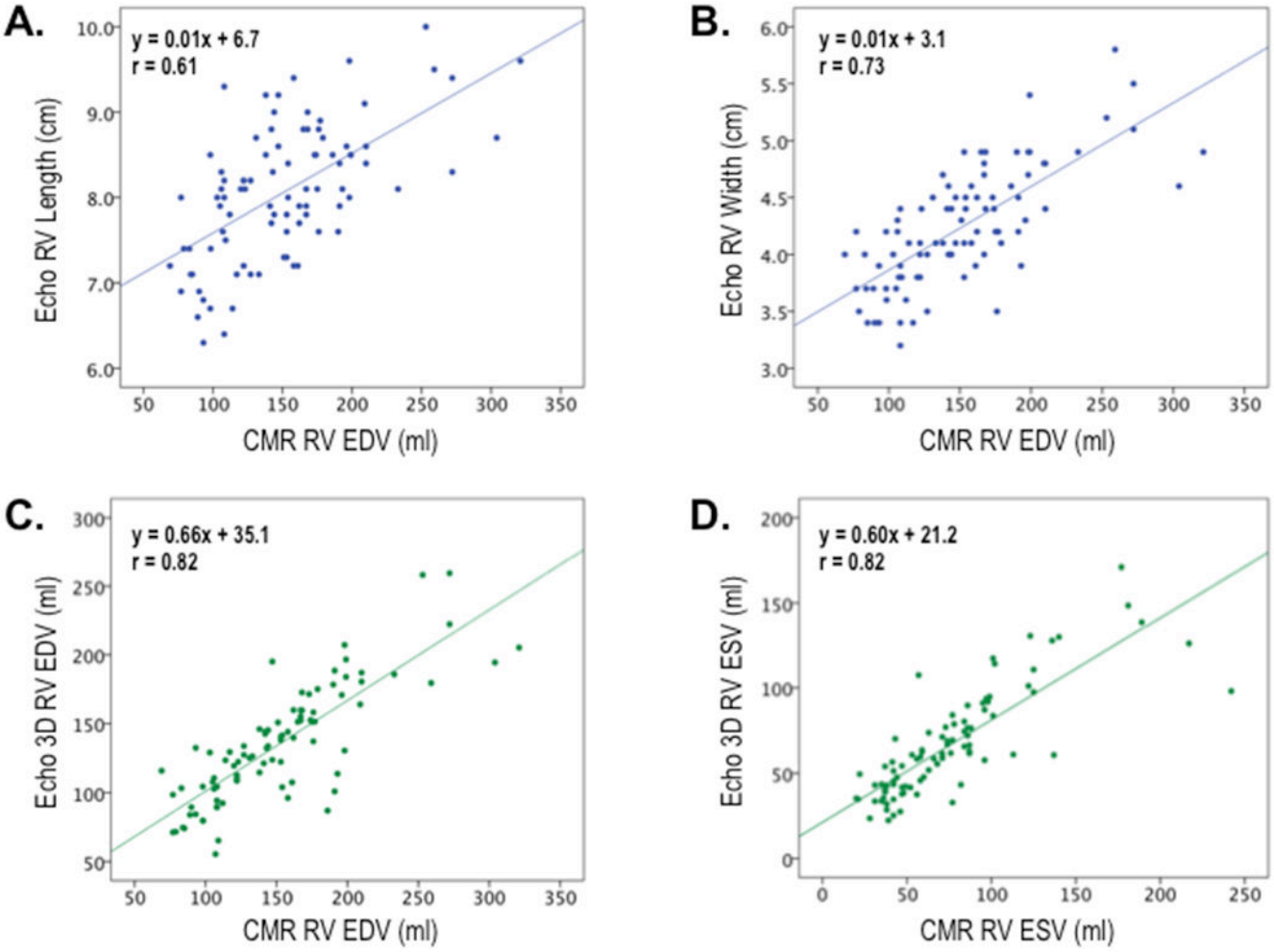

Figure 2. Echo Linear Dimensions in Relation to CMR RV Volume

Correlations between echo-derived linear dimensions (top, blue) and volumetric indices (bottom, green) in relation to CMR-derived RV volumes. Whereas all echo indices significantly correlated with RV volume on CMR ($p<0.001$), slightly higher correlations were yielded by volumetric compared to linear indices.

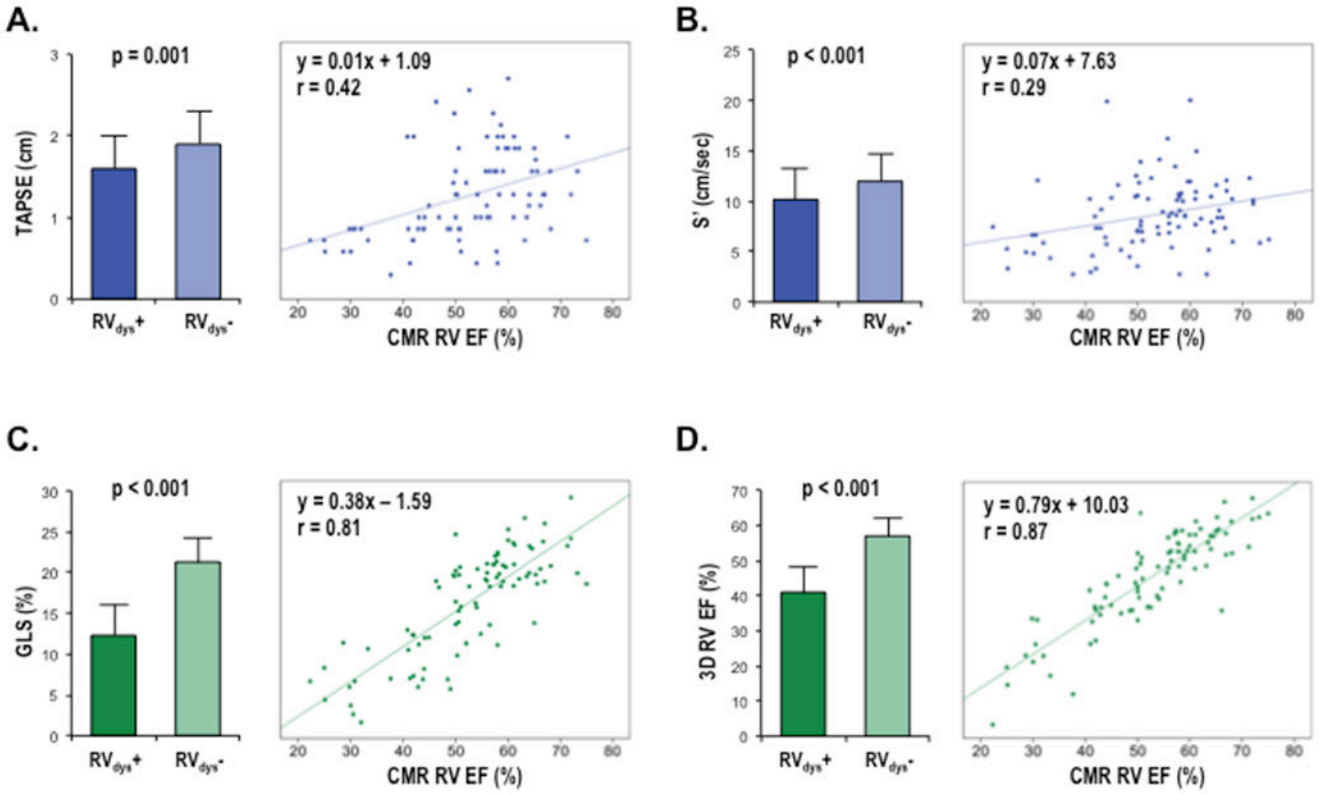

Figure 3. Echo Functional Indices in Relation to CMR-Evidenced RV Dysfunction

Echo-quantified RV functional indices (mean ± standard deviation) stratified by CMR-quantified RV_{DYS} (RVEF<50%) (left) as well as corresponding correlations of echo indices vs. CMR RVEF (right). Data shown for TAPSE (A), S' (B), GLS (C), and 3D echo (D).

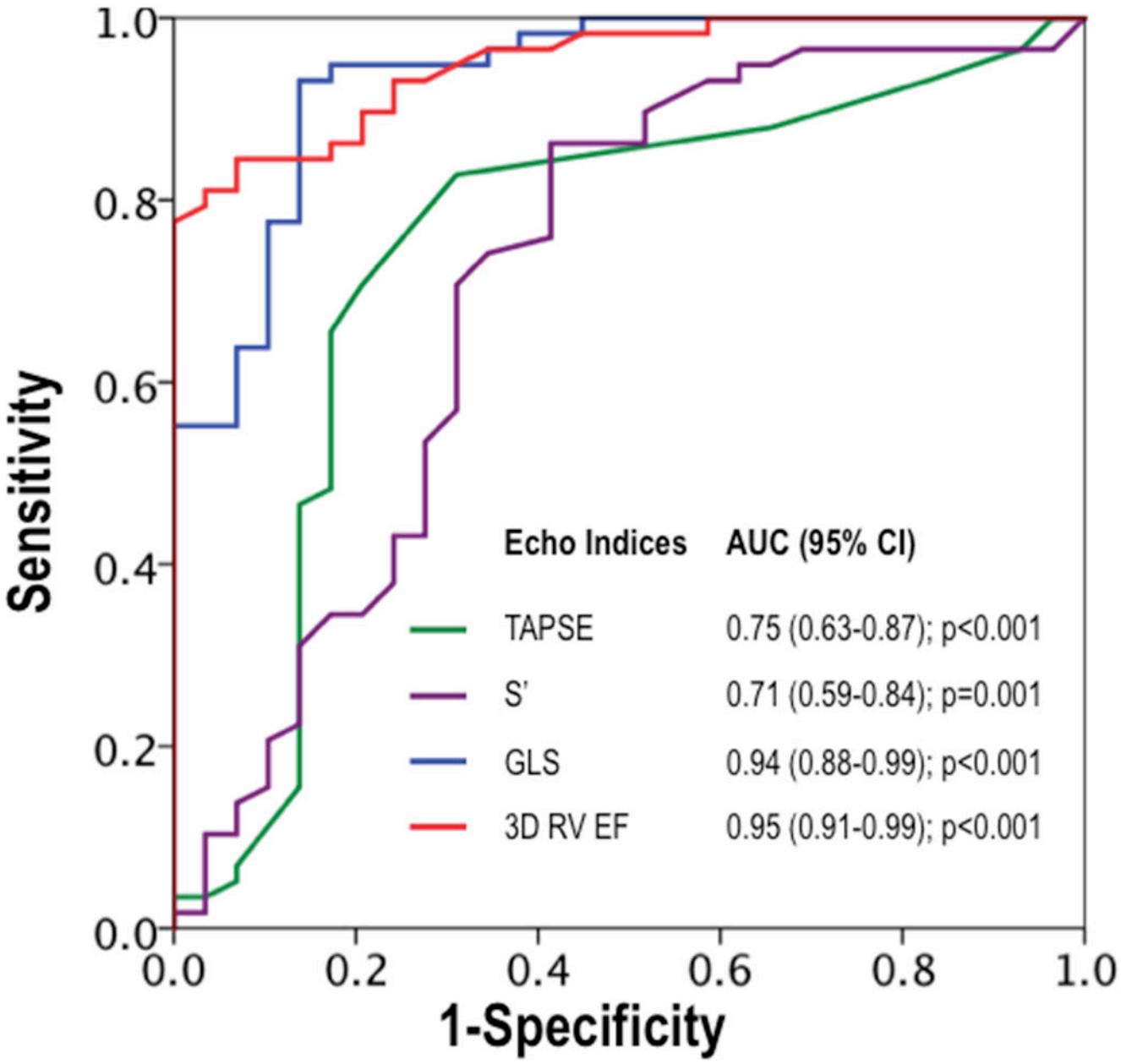

Figure 4. Diagnostic Performance of Echo Functional Indices for CMR-Evidenced RV Dysfunction

Receiver operating characteristics curves for conventional linear (TAPSE, S') and novel (GLS, 3D) echo indices in relation to RVEF<50% as established by the reference standard of CMR. Note that both GLS and 3D volumetric echo indices yielded higher but near equivalent overall diagnostic performance (as assessed via area under curve) compared to linear indices.

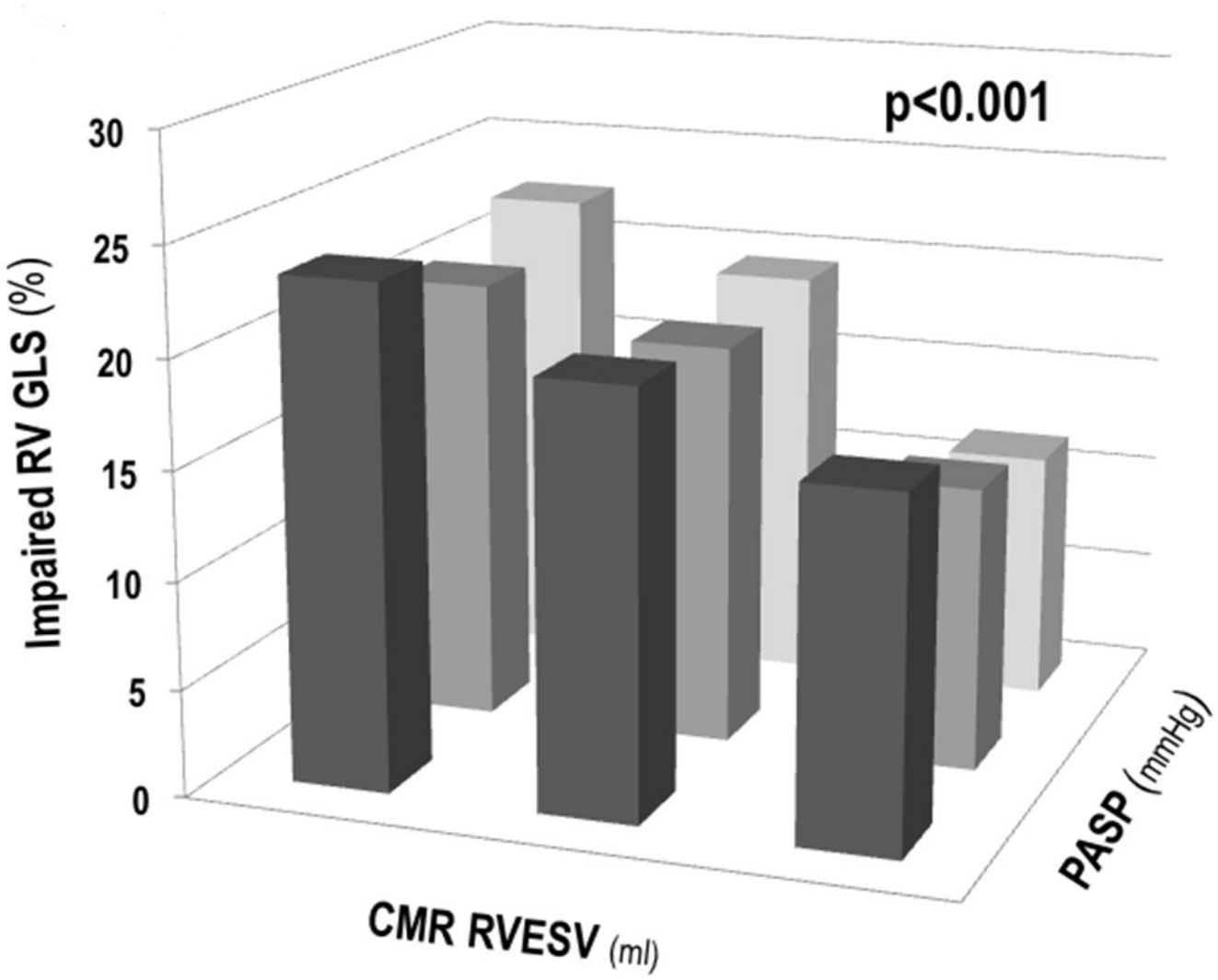

Figure 5. RV Global Longitudinal Strain in Relation to Wall Stress Determinants

Impaired RV GLS (y-axis) among groups partitioned by population-based tertiles of RV end-systolic volume (x-axis) and PA systolic pressure (z-axis). As shown, impaired GLS was primarily driven by increases in RV end-systolic volume across all three strata of PA systolic pressure.

Table 1.

Clinical and Imaging Characteristics

	Overall (n=90)	$RV_{dys}+$ * (n=29)	$RV_{dys}-$ (n=61)	p
CLINICAL				
Age (year)	68 ± 10	68 ± 11	67 ± 10	0.60
Male gender	81% (73)	90% (26)	77% (47)	0.15
Body surface area	1.9 ± 0.2	1.9 ± 0.2	2.0 ± 0.2	0.69
Heart rate	67 ±15	70 ± 14	65 ± 14	0.18
Systolic blood pressure	123 ± 17	123 ± 13	123 ± 19	0.93
Diastolic blood pressure	69 ± 11	70 ± 9	69 ± 12	0.78
Coronary Artery Disease Risk Factors				
Hypertension	79% (71)	66% (19)	85% (52)	**0.03**
Hypercholesterolemia	77% (69)	66% (19)	82% (50)	0.09
Diabetes mellitus	52% (47)	55% (16)	51% (31)	0.70
Tobacco use	61% (55)	66% (19)	59% (36)	0.55
Family history	24% (22)	24% (7)	25% (15)	0.96
Prior Myocardial Infarction	53% (48)	59% (17)	51% (31)	0.49
Prior Coronary Revascularization	77% (69)	79% (23)	75% (46)	0.68
Percutaneous Intervention	57% (51)	62% (18)	54% (33)	0.48
Coronary Artery Bypass Grafting	32% (29)	31% (9)	33% (20)	0.86
Cardiovascular Medications				
Beta-blocker	81% (73)	79% (23)	82% (50)	0.09
ACEI/ARB	63% (57)	76% (22)	57% (35)	0.09
Loop diuretic	42% (38)	59% (17)	34% (21)	**0.03**
HMG CoA-Reductase Inhibitor	81% (73)	83% (24)	80% (49)	0.78
Aspirin	89% (80)	86% (25)	90% (55)	0.72
Thienopyridine	42% (38)	45% (13)	41% (25)	0.73
Cardiovascular Symptoms				
Chest pain	56% (50)	66% (19)	51% (31)	0.19
Dyspnea	67% (60)	83% (24)	59% (36)	**0.03**
NYHA Class (1/2/3/4)	(56%/26%/11%/7%)	(28%/38%/21%/14%)	(69%/21%/7%/3%)	**<0.001**
CARDIAC MORPHOLOGY/FUNCTION (CMR)				
Right Ventricle				
Ejection fraction (%)	52.8 ± 12.0	38.9 ± 8.2	59.4 ± 6.6	**<0.001**
End-diastolic volume (ml) *	151.2 ± 51.4	179.2 ± 55.8	138.0 ± 43.7	**<0.001**
End-systolic volume (ml) *	74.8 ± 42.4	111.9 ± 48.9	57.2 ± 23.9	**<0.001**
RV myocardial mass (g)	29.1 ± 10.4	32.3 ± 8.6	27.6 ± 10.9	**0.046**
(g/m^2)	14.9 ± 5.0	16.9 ± 5.1	14.0 ± 4.7	**0.009**
Relative mass (g/ml)	0.20 ± 0.05	0.18 ± 0.03	0.20 ± 0.05	0.08
End-diastolic length (cm)	7.4 ± 1.2	8.0 ± 1.0	7.1 ± 1.2	**0.002**

	Overall (n=90)	$RV_{dys}+^{*}$ (n=29)	$RV_{dys}-$ (n=61)	p
End-diastolic width (cm)	4.2 ± 0.7	4.5 ± 0.7	4.1 ± 0.7	**0.009**
Left Ventricle				
Ejection fraction (%)	43.8 ± 14.9	31.8 ± 11.2	49.5 ± 13.1	**<0.001**
End-diastolic volume (ml)	201.2 ± 63.8	236.2 ± 57.0	184.5 ± 60.4	**<0.001**
End-systolic volume (ml)	119.6 ± 62.1	164.4 ± 54.8	98.3 ± 53.7	**<0.001**
LV myocardial mass (g)	158.7 ± 47.7	172.3 ± 37.6	152.2 ± 50.8	0.06
(g/m^2)	81.1 ± 21.2	89.3 ± 18.0	77.2 ± 21.7	**0.01**
End-diastolic diameter (cm)	6.0 ± 0.8	6.3 ± 0.5	5.8 ± 0.8	**0.004**
ECHOCARDIOGRAPHY				
Mitral Regurgitation				
Severity grade (1–4)	1.6 ± 0.9	2.1 ± 1.0	1.3 ± 0.7	**<0.001**
Regurgitant fraction (%)	37.3 ± 14.7	42.2 ± 15.3	33.5 ± 13.2	**0.02**
Pulmonary arterial pressure (mmHg)	37.8 ± 15.0	43.5 ± 15.5	34.6 ± 13.8	**0.01**
Pulmonary hypertension[§]	51% (37)	69% (18)	40% (19)	**0.02**
Advanced pulmonary hypertension[°]	15% (11)	31% (8)	6% (3)	**0.01**

[*] RV dysfunction defined as RVEF<50%.

[§] Pulmonary hypertension defined as PASP>35 mmHg.

[°] Advanced pulmonary hypertension defined as PASP>50.

Data presented as mean ± standard deviation (data in parentheses refer to range for each respective variable).

Table 2.

Tissue Based Markers of RV Dysfunction

	Overall (n=90)	RV_{dys} + (n=29)	RV_{dys} – (n=61)	p
Myocardial Infarct Size				
Global MI (%)	10.4 ± 10.0	13.2 ± 9.0	9.0 ± 10.3	0.06
Anterior MI (%)	1.2 ± 2.1	1.2 ± 1.7	1.3 ± 2.3	0.98
Lateral MI (%)	3.6 ± 5.2	4.1 ± 4.9	3.3 ± 5.4	0.47
Inferior MI (%)	3.7 ± 5.3	5.6 ± 6.5	2.8 ± 4.5	**0.04**
Myocardial Ischemia Burden*				
Global Ischemia	12.9 ± 9.1	16.5 ± 11.1	11.5 ± 7.9	**0.03**
Anterior Ischemia	2.2 ± 2.8	2.8 ± 2.8	2.0 ± 2.8	0.26
Lateral Ischemia	3.0 ± 3.3	4.0 ± 4.0	2.6 ± 2.9	0.10
Inferior Ischemia	5.8 ± 4.5	7.6 ± 4.6	5.1 ± 4.3	**0.03**

*Stress perfusion performed in 82% (n=74) of patients.

Table 3.

CMR-Evidenced RV Dysfunction in Relation to 2D, Strain and 3D-Based Echo Indices

	Overall (n=90)	**RV_{dys} + (n=29)**	**RV_{dys} − (n=61)**	**p**	**r**	**p**
TAPSE (cm)	1.8 ± 0.4	1.6 ± 0.4	1.9 ± 0.4	**0.001**	0.416	**<0.001**
S' (cm/sec)	11.4 ± 3.0	10.2 ± 3.2	12.0 ± 2.7	**0.009**	0.287	**0.006**
RV GLS (%)	18.3 ± 5.6	12.3 ± 4.3	21.2 ± 3.5	**<0.001**	0.805	**<0.001**
3D RVEF (%)	52.3 ± 10.1	41.4 ± 8.4	57.4 ± 6.1	**<0.001**	0.872	**<0.001**

Table 4.

Diagnostic Performance of Echo Parameters for RV Dysfunction

	Cutoff	Sensitivity	Specificity	Accuracy	PPV	NPV
TAPSE	1.6 cm	69%	84%	79%	67%	85%
S’	10 cm/s	59%	82%	74%	61%	81%
GLS	20%	90%	79%	82%	67%	94%
3D RVEF	50%	83%	85%	84%	73%	91%

Table 5.

Multivariate Regression for RV GLS

	Univariate Regression		Multivariate Regression *Correlation coefficient = 0.51, p<0.001*	
Variable	**Odds Ratio (95% Confidence Interval)**	**p**	**Odds Ratio (95% Confidence Interval)**	**p**
PA Systolic Pressure*	−1.55 (−2.37 – −0.72)	**<0.001**	−0.45 (−1.23 – 0.34)	0.26
RV End-Systolic Volume*	−0.85 (−1.07 – −0.64)	**<0.001**	−0.90 (−1.19 – −0.61)	**<0.001**
RV Myocardial Mass*	−1.90 (−2.97 – −0.82)	**0.001**	.72 (−0.49 – 1.92)	0.24
	Univariate Regression		**Multivariate Regression** *Correlation coefficient = 0.49, p=0.005*	
Variable	**Odds Ratio (95% Confidence Interval)**	**p**	**Odds Ratio (95% Confidence Interval)**	**p**
PA Systolic Pressure*	−1.30 (−2.14 – −0.47)	**0.003**	−1.03 (−2.04 – −0.02)	**0.045**
3D RV End-Systolic Volume*	−0.60 (−0.87 – −0.34)	**<0.001**	−0.43 (−0.84 – −0.02)	**0.04**
RV Wall Thickness	−2.29 (−26.70 – 22.13)	0.39	12.66 (−12.03 – 37.34)	0.31

* per increments of 10 (ml, mg, mmHg respectively)